



# Design, Construction, and Back-Analysis of a Deep Underground Parking Garage in an Urban Environment

**Seppe Creten**, Engineer, BESIX Engineering Department (Brussels, Belgium); email: [seppe.creten@besix.com](mailto:seppe.creten@besix.com)

**Hans Verbraken**, Engineer, BESIX Engineering Department (Brussels, Belgium) and Department of Civil Engineering, KU Leuven (Leuven, Belgium); email: [hans.verbraken@besix.com](mailto:hans.verbraken@besix.com)

**Stijn François**, Assistant Professor, Department of Civil Engineering, KU Leuven (Leuven, Belgium); email: [stijn.francois@kuleuven.be](mailto:stijn.francois@kuleuven.be)

**Christophe Bauduin**, Technical Director, BESIX Engineering Department (Brussels, Belgium) and Department of Civil Engineering, KU Leuven (Leuven, Belgium); email: [christophe.bauduin@besix.com](mailto:christophe.bauduin@besix.com)

**ABSTRACT:** *This paper studies the deformations caused by a deep excavation in an urban environment. The case study involves an underground parking garage in the historical center of the Dutch town of Leiden, characterized by a high water level and soil layers containing clay, silt, and peat. The design of this kind of structure in these conditions is usually accompanied by a lot of uncertainties. Therefore, a thorough comparison of the structure's expected behavior and its actual behavior is very useful to improve the accuracy of future calculations.*

*With this in mind, the predictions based on different calculation methods are compared to both inclinometer-measured deformations of the garage itself and settlements of historical buildings around the excavation. Both a back-analysis and a sensitivity analysis are carried out, taking into account the most important influence factors for the excavation. Based on this analysis, recommendations are made for increased accuracy of future calculations.*

**KEYWORDS:** Deep excavations, Inclinometers, Diaphragm Walls, Dewatering, Urban Environment, Back-analysis

**SITE LOCATION:** [Geographic Database](#)

## INTRODUCTION

Due to increasing population numbers, the available free construction space decreases. Therefore, there is an increasing need for underground constructions. This is not as simple as it seems, however, since underground constructions have their own inherent set of risks and design difficulties. As a result, geotechnical installation techniques for underground constructions are under continuous development. These techniques are accompanied by advanced calculation methods in support of the design.

Generally speaking, two types of displacements are of importance for excavations in urban environment. First, there is the horizontal displacement of the retaining structure itself; this displacement is typically limited to a certain value by a local standard. Secondly, there are the settlements behind the retaining structure. These settlements are of particular importance for excavations in urban areas since they determine the possible damage to nearby buildings and utility lines. As a result, these settlements are the input parameters for many methods to predict damage to buildings, ranging from early empirical methods like the method of Skempton and MacDonald (1956) or the LTSM method by Burland and Wroth (1974) to modern-day calculations using the finite element method to assess possible damage to nearby buildings.

Due to the uncertainties that accompany large underground constructions and the importance of the displacements caused by them, these works are often accompanied by in-situ measuring and monitoring programs. The goal of these monitoring campaigns is, in most cases, to be able to react in time if the structure behaves unexpectedly (in practice, this would most likely be if the deformations exceed a certain boundary) and failure could be imminent.

Submitted: 15 January 2021; Published: 10 December 2021

Reference: Creten S., Verbraken H., François S., and Bauduin C. (2021). Design, Construction, and Back-Analysis of a Deep Underground Parking Garage in an Urban Environment. International Journal of Geoengineering Case Histories, Volume 7, Issue 1, pp. 113-136, doi: 10.4417/IJGCH-07-01-06

Once the construction is completed and the deformations don't come close to the imposed boundaries, the measured data are archived and usually nothing else is done with them. This is a lost opportunity, since both the engineering models used in practice (from the designer's side) and a lot of measured data are already available to validate the engineering models. This would not only allow us to check how safe the design is based on the margin between measured and calculated data, but also to make the design more economical (by decreasing this margin). In this way, valuable lessons for the future can be learned.

In literature, examples can be found where measurements and calculations for deep excavations are compared, like the cases described by op de Kelder (2015) or Hsiung and Dao (2014). Another example of such a comparison is the project "Le Carrefour" in Leiden (NL), as described by Rooduijn (2010). This latter project is of particular interest since the measured horizontal deformations were significantly lower than the calculated values. This is thus an interesting case from a more economic point of view, since further optimizations should be possible.

With all this in mind, the construction of an underground parking garage at the site of the Garenmarkt in the Dutch city of Leiden appeared to be a very interesting object of study, given that it combined all the aforementioned properties. Both advanced installation techniques were used and an extensive measuring campaign (measuring both the deflection of the retaining walls and settlements around the excavation) was executed due to its proximity to historically valuable buildings. The parking garage also had to cope with some typical problems that can be found while building underground in Dutch cities, like a high water level, rather soft soils, and (here specifically) a number of important historical buildings right next to the excavation site. Finally, there still appeared to be quite some options to make the design more economical.

The three case studies mentioned from literature focus mainly on the same aspect of modeling a geotechnical structure: namely, the constitutive model and the used mesh. All three demonstrate the superiority of hardening soil models with the small strain stiffness of "regular" hardening soil models or the Mohr-Coulomb model, and this for different soil types. Since this is well established, this paper does not dwell on this but instead focuses on other choices made during the design, such as how to model the walls, the struts, and so forth. This paper is based on a more extensive study in the context of a master's thesis by Seppe Creten (2020).

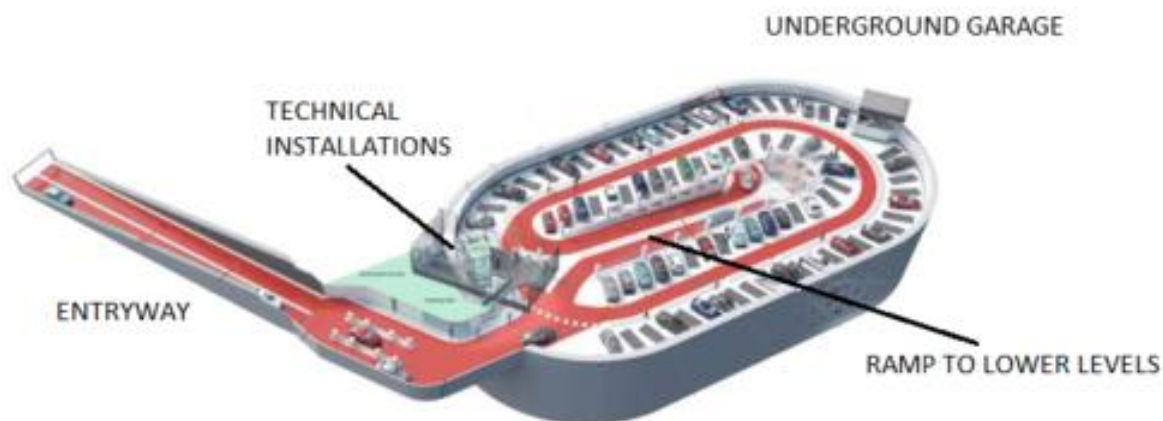


*Figure 1. Three-dimensional view of the parking garage underneath the Garenmarkt.*

Figure 1 provides a three-dimensional view of the parking garage. As shown in the figure, this particular parking garage has the shape of a hippodrome. Vehicles can enter through the entryway shown on the left. The ramp to reach the lower levels (which are five in total) is situated in the center of the parking garage.



## PROJECT DESCRIPTION

### Soil Description

The city of Leiden (NL) is located in a polder area, which is crossed by the Old Rhine River and several canals (also near to the Garenmarkt). This presence of waterways results in a high groundwater level only 60 cm below the surface (itself located at a level of -1 mNAP (the vertical datum in the Netherlands)).

The different soil layers and their most important parameters encountered at the Garenmarkt are given in Table 1. Below a level of -13.2 mNAP, the soil consists of sturdy sand layers. Above this level, the soil is of a lesser quality, consisting of weaker silty sands, interrupted by a clay layer 1.45 m underneath the surface and a 2 m thick layer of peat about 10.8 m deep beneath the surface.

The soils closest to the surface are Holocenic, whereas the formation of Boxtel and Kreftenheye are found in deeper soil layers.

Table 1. Soil parameters.

Top level [mNAP]	Geotechnical entity	$\gamma_{wet}$ [kN/m <sup>3</sup> ]	$\gamma_{sat}$ [kN/m <sup>3</sup> ]	$\phi'$ [°]	$c'$ [kPa]	$c_u$ [kPa]
-0.40 (surface)	Silty sand (1)	17	19	25	-	-
-1.85	clay (1)	16	16	25	2	20
-4.00	Sand (1)	17	19	30	-	-
-6.00	Silty sand (2)	17	19	27	-	-
-10.00	Silty sand (1)	17	19	25	-	-
-10.40	Sand (1)	17	19	30	-	-
-11.00	Silty sand (2)	17	19	27	-	-
-11.20	Peat	13	13	15	7	60
-13.20	Sand (2)	18	20	33	-	-
-19.30	Sand (3)	19	21	35	-	-
-24.90	Sand (2)	18	20	33	-	-
-28.00	Sand (3)	19	21	35	-	-

### Geometry

Viewed from above, the parking garage has a shape resembling a hippodrome. As a result, the central part of the excavation is supported by straight walls, while the walls at the two ends are curved. The central part is roughly square shaped, with sides of 40 m long. The walls of the excavation for this section consist of diaphragm walls with a width of 1 m. The two semi-circles at the sides have radii of nearly 20 m, and the thickness of the diaphragm walls here is 0.8 m. The exact dimensions can be found in Figure 2.

On the bottom right of Figure 2, the entryway can be seen where the soil is not supported by diaphragm walls but by less stiff sheet-pile walls.

The soil itself is retained by concrete diaphragm walls. The top of these walls is situated at a level of -0.4 mNAP, and the bottom of the diaphragm walls is situated at -24 mNAP. The bottom level of the excavation itself is at a level of -18.2 mNAP. This is shown in Figure 3.

### General Principle of the Realization

In the first phase of the realization, the diaphragm walls are installed. In the straight part, these walls are horizontally supported by struts at different levels. The curved part of the structure does not use any horizontal form of support; the curved walls work as a barrel vault placed on its side, transferring the axial compression in the curved walls to the straight walls in the central part.

After the walls are in place, the beams that serve to carry the roof of the parking garage are constructed and serve as the uppermost strut level. After the construction of the concrete beams, the real excavation begins. This excavation happens top-down, from the surface.

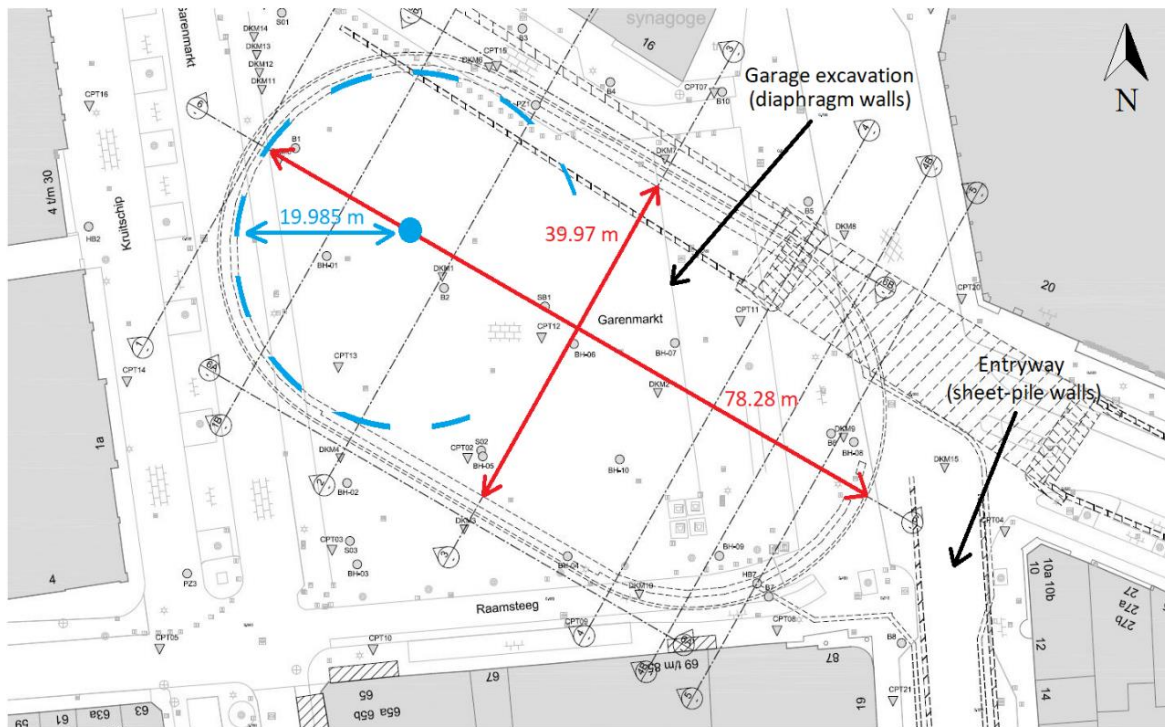


Figure 2. Dimensions of the excavation.

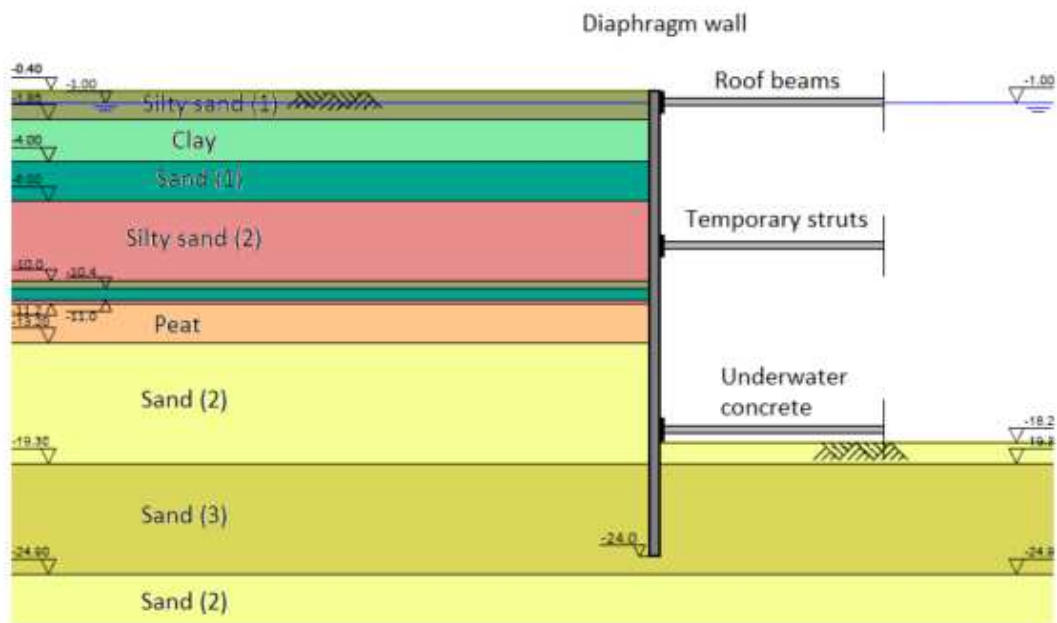


Figure 3: Cross-section of the excavation.



An important boundary condition for this excavation is the high groundwater level. Since the soil at the bottom of the excavation is sandy and permeable, keeping the excavation dry by pumping the water out is very difficult. Therefore, the excavation is done without dewatering.

As the wet excavation progresses, more struts are added at various levels. The first strut is a temporary steel frame at -8.25 mNAP. The third strut level is situated at -17.58 mNAP. This group of struts is not a collection of beams, as the two uppermost struts, but is actually the floor of the parking garage. This floor is made of (underwater) concrete, and is poured when the excavation reaches its deepest level. To prevent uplift once the excavation is set dry, the floor is held in place by anchor-piles and barrettes (a barrette is a single diaphragm wall panel that serves as rectangular foundation pile).

When all the walls, struts, and the impermeable floor are in place, the water is pumped out of the excavation pit and the permanent structure is constructed. First, the permanent floor slab is installed. This takes over the function of the (unreinforced) underwater concrete slab and is also connected to the anchor piles. The different (permanent) floors are subsequently added, of which two will serve as a strut for the retaining walls and thus replace the temporary steel frame.

## DESIGN CALCULATIONS

### Expected Behavior of the Structure

Due to the hippodrome shape of the excavation, three distinct “types” of behavior can be distinguished:

- 2D Plane Strain Behavior. In the straight walls of the rectangular part of the excavation, the behavior of the walls represents two-dimensional plane strain conditions and can therefore be calculated (or at least be well approximated by) using two-dimensional methods.
- 2D Axisymmetric Behavior. This behavior should occur in the semi-circular part of the excavation; the subsequent displacements can be found by two-dimensional calculations.
- 3D Transitional Behavior. The displacements in the two two-dimensional zones are not the same, and as a result there should be a zone of transition between the two zones where there is a smooth change from the plane strain to the axisymmetric displacements. Quantifying these displacements asks for a three-dimensional approach of the calculations.

### Calculation Software and Methods

The different calculations that have been carried out can be categorized as spring models and finite element (FE) models.

- Elastoplastic Spring Models. These models replicate the soil as a series of uncoupled elastoplastic springs. These springs are defined by a rather simple force-displacement relationship. The non-linear spring stiffness varies with horizontal displacement. The maximal force is capped at the passive earth pressure; the minimal force is capped at the active earth pressure. This kind of model only gives 3 forms of output; bending moments, shear forces and horizontal displacements. Spring model calculations were carried out using the D-sheet Piling software (only two-dimensional).
- Finite Element Method. FEM models allow us to consider much more complicated stress-strain relationships than do the spring models. In comparison to the spring model, a FEM model also allows us to calculate the vertical and horizontal displacements behind the wall. This is a very important asset in this case, since displacements of nearby buildings need to be assessed. For the FEM calculations, the software PLAXIS (both two- and three-dimensional) was used, applying a Hardening Soil constitutive model with small-strain stiffness (HS Small).

Two different three-dimensional models have been made: one model only considers the main excavation pit (the “hippodrome”), while the second model also considers the entrance. This second model is asymmetric and creates asymmetric behavior of the building pit.

As a way of checking how reasonable the results are, a quick cross-check has been carried out with some typical empirical correlations, like the ones from: Clough & O’Rourke (1990), who estimate the horizontal displacement of the wall at 0.2%



of its height; the correlation from Moorman (2004), who gives a slightly higher value of 0.25% of the wall's height; and the datasets of Long (2001), who gives 0.21%.

The value given by Clough & O'Rourke is based on data from different wall types, as shown in Figure 4. In this figure, it is clear that, generally speaking, the diaphragm walls are stiffer than most of the other wall types. Therefore, an extra correlation, based solely on the diaphragm walls (Figure 5), is also composed (deflection is 0.12%H). In the rest of this text, this correlation is denoted as "Clough & O'Rourke\*".

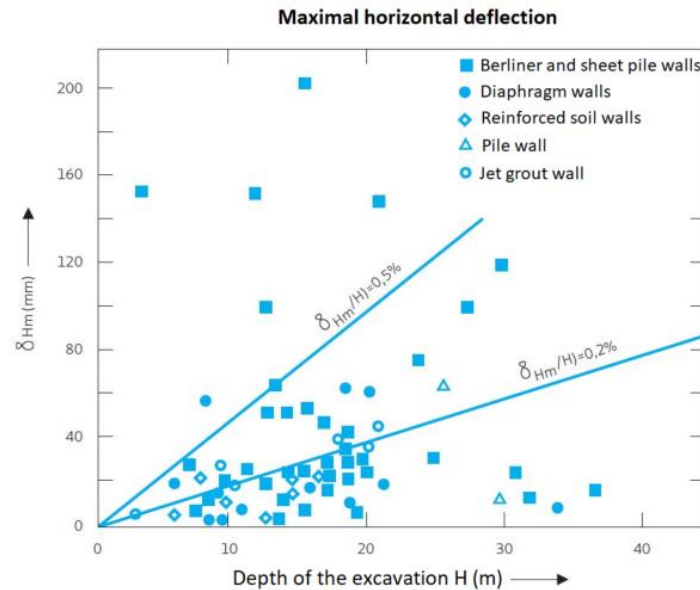


Figure 4. Dataset used by Clough & O'Rourke to determine the ratio of deflection to height of the wall, COB-report F530 (Korf et al. 2012).

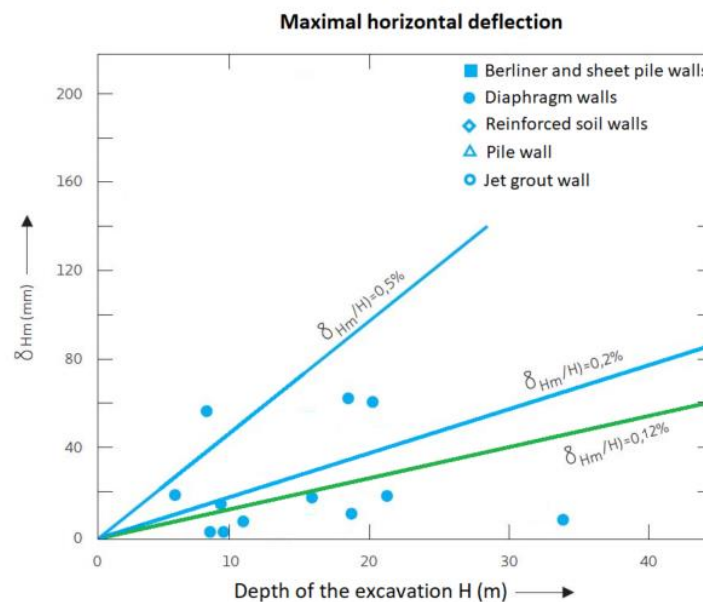


Figure 5. Dataset of Clough & O'Rourke showing only the diaphragm walls; adaption from COB-report F530 (Korf et al. 2012).



It is important to note that some of the used calculation models assume a two-dimensional situation where the wall is sufficiently long for the edge effects to have disappeared towards the center. These edge effects make the construction stiffer (for example, a perpendicular wall that serves as some sort of strut). This effect has been studied by Ou et al. (1996), who define the *plane strain ratio* (PSR) as:

$$PSR = \frac{u_{3D}}{u_{plane\ strain}} \quad (1)$$

The PSR is herein based on the ratio of the length of the primary wall (whose deflection is studied) and the secondary wall (which serves as a support). The PSR also depends on how far the considered point is removed from the secondary wall. For the Garenmarkt, the PSR based on the literature equals 0.55 at the location where the vertical displacement of the diaphragm wall is measured.

### Calculated Displacements

For the straight walls, the displacements are shown in Figure 6. Agreement is found between the two-dimensional plane strain calculations. The PLAXIS calculation predicts 27.2 mm, while the D-sheet piling predicts 27.6 mm. In comparison with the three-dimensional calculation, there is a small difference since the PLAXIS 3D calculation predicts a value of  $u_a$  equal to 24.0 mm for the symmetric model and 23.3 mm for the asymmetric one.

The three-dimensional calculations give a lower value than the two-dimensional ones; this makes sense since the curved walls at the edges prohibit displacements. The plane strain approach assumes, however, that the entire wall deforms the same. This edge effect is expected to reduce the deformation at the center of the straight wall by 12% as compared to a real plane strain situation.

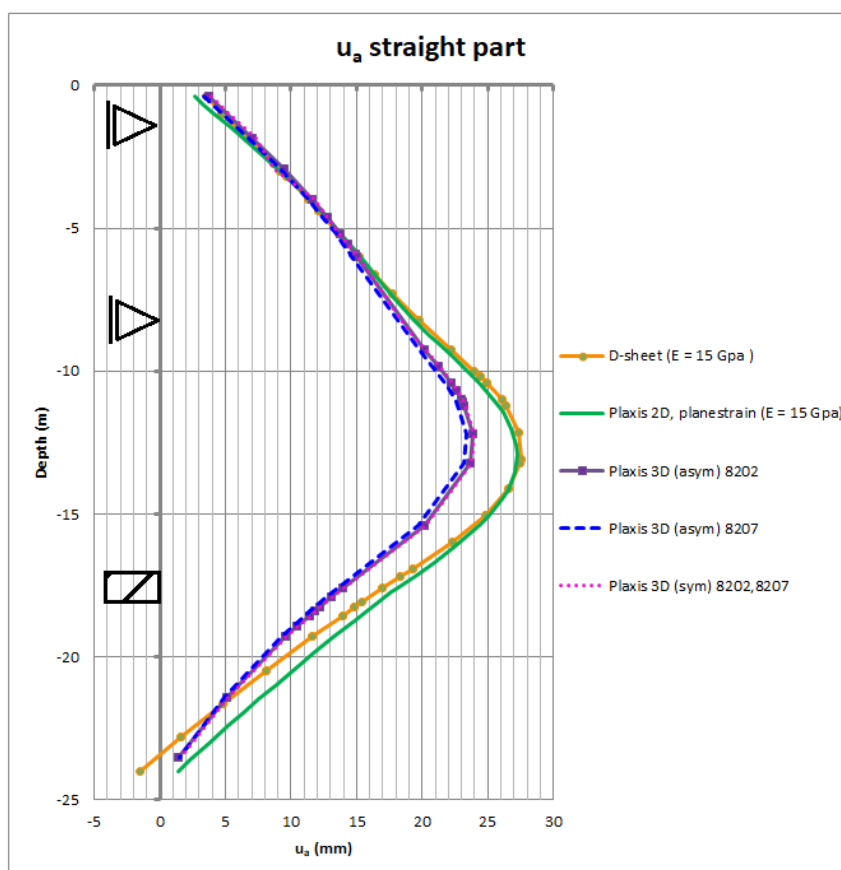


Figure 6. Displacements calculated for the straight walls.



For the straight walls, the results of the different calculations (springs, FE, and empirical correlations) are given in Table 2. A peculiar observation made in this table is that the values using the PSR, as defined by Ou et al. (1996), are less than those found in the three-dimensional calculations. This is due to the fact that the “secondary wall” is not a straight perpendicular wall to the primary one, but rather a wall that is curved and therefore is much more flexible. In this case, the PSR based on the self-made PLAXIS model equals 0.875 instead of the 0.55 found by Ou et al. (1996).

On the other hand, using the “standard” correlations gives much larger values than the more precise calculations. An exception is the self-made correlation based on the data of Clough & O’Rourke (1990); this correlation gives a result rather similar to the PLAXIS 3D results.

*Table 2. Results of the different horizontal displacement calculations for the straight walls of the excavation.*

<i>Method</i>	<i>2D prediction</i>	<i>3D prediction or 2D x PSR</i>
Clough & O’Rourke (1990)	-	36.0
Clough & O’Rourke*	-	21.6
Moorman (2004)	-	45.0
Long (2001)	-	37.8
D-sheet piling	27.6	15.2
PLAXIS 2D	27.2	15.0
PLAXIS 3D (sym)	-	24.0
PLAXIS 3D (asym)	-	23.3

For the axisymmetric and the transition zones, the calculated displacements are shown in Figure 7. For these predictions, no spring model was used. For the axisymmetric zone, a two-dimensional FE calculation was carried out, as well as calculations with the symmetric and asymmetric three-dimensional model. In the transition zone, only three-dimensional calculations were carried out.

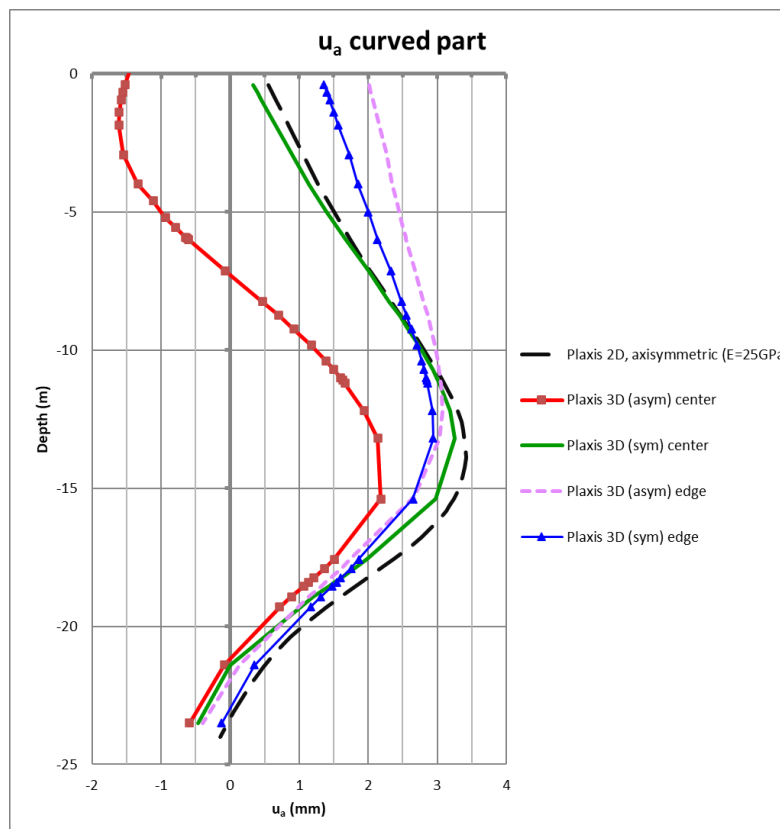


*Figure 7. Displacements in the axisymmetric and transition zones.*





When the influence of the excavation of the entrance is not considered, the three-dimensional calculation shows that the transition effects from the straight edges are more or less gone in the center of semi-circular wall. This is shown by the similarity of the axisymmetric 2D results with the 3D results.

The most important influence of the transition effects can be found by comparing the results of the center of the semi-circle to the edge of the semi-circle. The maximal displacement is roughly the same for both; the main difference is the displacement of the top of the diaphragm wall. This part of the wall moves more into the pit closer to the straight walls. The values of the top displacements near the edge of the semi-circle are predicted to be in the 2 mm to 3 mm range, which is the same displacement as predicted for the straight part. The maximal displacements over the entire wall are in the range of 3 mm to 4 mm; this is small in comparison to the maximal displacements for the straight walls, which were situated around 25 mm (depending on the used method).

Apart from the displacements of the walls (Which were interwoven with the forces who govern the design of the construction), another important design aspect is the settlement of the soil around the structure. These settlements are one of the primary reasons for the damage caused to the surroundings of the excavation. In the case of the Garenmarkt, which is surrounded by lots of ancient buildings—many of which are listed as Dutch national heritage sites (*Rijksmonuments*)—these settlements are perhaps an even more significant design aspect than the design of the excavation itself. This especially true for those placed on shallow foundations, like the Leiden Synagogue.

The total settlements around the excavation can be attributed to the following three causes:

- Excavations for removing sewage pipes. The old pipes ran through the location of the parking garage and have to be moved. The upper limit of these settlements is quantified at 5 mm.
- Excavation and draining of the actual parking garage. The settlements around the excavation pit can only be calculated precisely by a FE calculation. Results of this calculation are shown graphically in Figure 8. Based on the PLAXIS calculation, the maximal settlements can be expected next to the straight walls of the parking garage. This is not surprising, since it is the straight walls that deform the most. The maximal settlement is expected at the synagogue (settlement of 15.2 mm).
- Excavation of the entrance. Only a portion of the entrance is put into the model of the excavation pit. To calculate these settlements, a separate model was created, resulting in a maximal settlement of 8.6 mm.

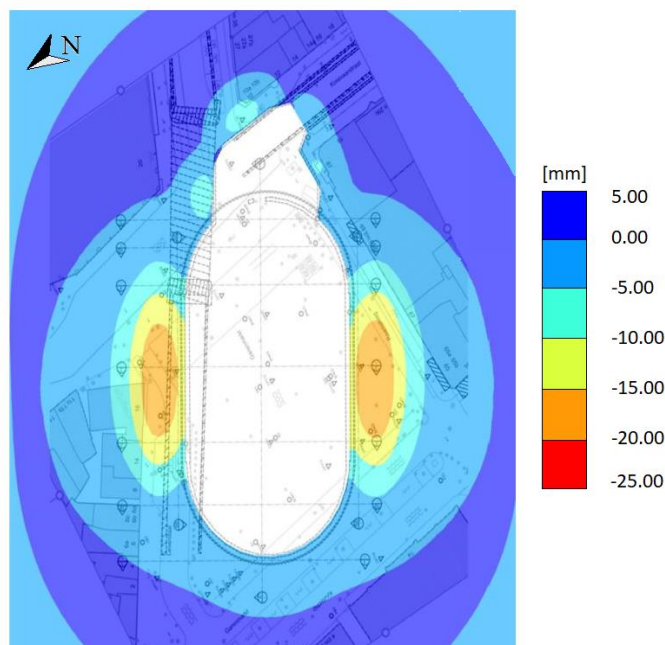


Figure 8. Calculated settlements from the asymmetric PLAXIS 3D model.



The upper limit of the total settlement (calculated as the sum of the three amounts given above) is shown graphically in Figure 8. This figure shows that maximal settlements are expected at the synagogue (mainly due to the influence of the excavation of the garage itself) and the building at the edge of the Korevaarstraat (due to the cumulative effect of the three reasons of settlement).

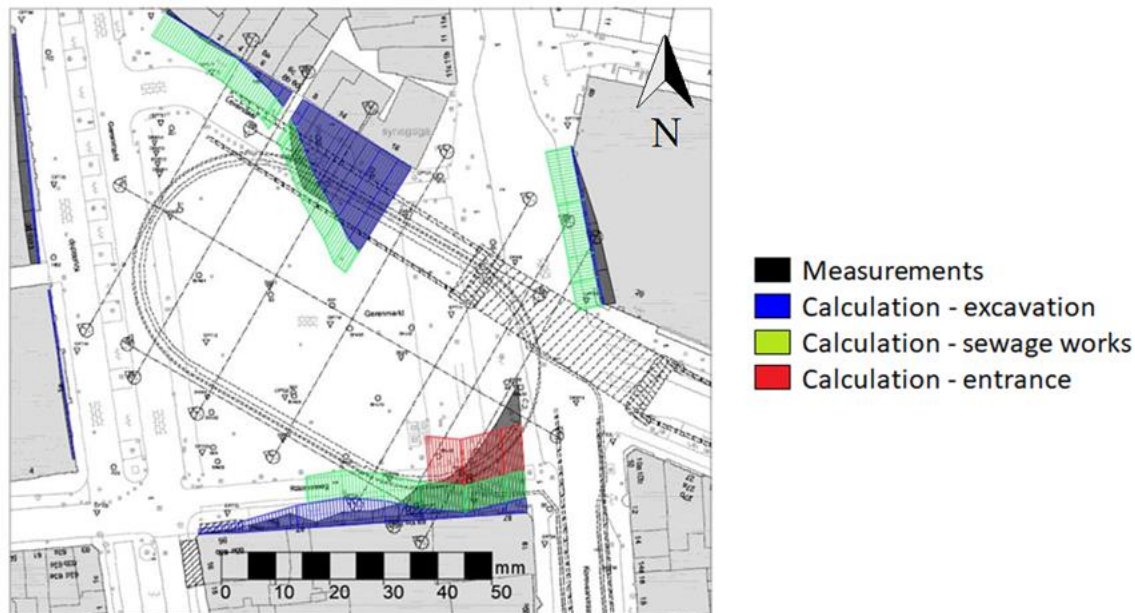


Figure 8. Upper limit of the total expected settlements as a sum of sewage works (green), excavation of the garage (blue), and excavation of the entrance (red). The measurements are plotted in black.

## IN-SITU MEASUREMENTS DURING CONSTRUCTION

### Measured Parameters

At different locations of the excavation, the horizontal displacements of the diaphragm walls were measured. These displacements are composed of two different components:

- $u_a$ : the horizontal displacement perpendicular to the plane of the diaphragm wall; these displacements are defined as positive when the wall moves towards the excavated site.
- $u_b$ : the horizontal displacement parallel to the plane of the diaphragm wall; these deformations are defined as positive when the movement is towards the center of the eastern semi-circle.

The measurements of these displacements have been conducted at six distinct locations around the excavation, and each of these has received its own reference number:

- 8001: Placed near the center of the southern straight wall, the locations were measured behind the diaphragm wall; as a result, the displacements of the soil behind the excavation can be monitored.
- 8002: Done behind the northern wall instead of the southern one, this is another location that measured the soil displacement behind the wall.
- 8202: Located in front of Location 8001 on the southern straight wall, this measured the displacement of the diaphragm wall itself.

- 8204: Situated on the interface between the straight wall and the curved wall; these measurements should be useful to study the change from plane-strain behavior in the straight part of the wall to axisymmetric behavior in the curved part.
- 8206: Located near the center of the curved wall; these measurements should be consistent with the axisymmetric calculations.
- 8207: Located in front of Location 8002 on the northern straight wall; measured the displacement of the diaphragm wall itself.

To clarify the position of the different measurements, Figure 10 shows the different locations on a satellite image of the excavation.

The vertical settlements of the buildings surrounding the square are also important types of displacement for the Garenmarkt. These are measured on the edges of each building (and also on intermediate points for the larger buildings).

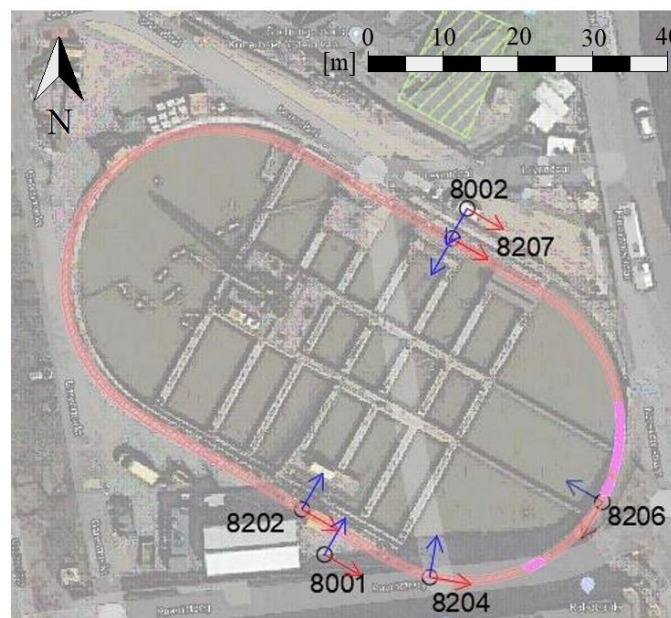


Figure 9. Locations of the different measurements of the horizontal displacements, where  $u_a$  is perpendicular to the wall and  $u_b$  is parallel to the wall.

## Measuring Equipment

The horizontal displacements were measured using electrolevel in-place inclinometers (EL-IPI). These inclinometers were placed with a vertical interdistance of 50 cm and measured the inclination at their respective location. As such, the relative displacements of the inclinometers could be calculated.

The result of this calculation is the relative displacement of all the inclinometers. In order to find the absolute displacement, a fixed point of reference is needed. A first option is to use the toe of the diaphragm wall as the reference point, since it is reasonable to assume that the toe-movement is rather limited. Another (and more reliable) option is to measure the displacement of one of the inclinometers and use that as reference point. For the Garenmarkt, this second option was used, the location of the uppermost inclinometer was measured with a total station. As a result, the highest inclinometer could be used as reference point.

The maximal error on the inclinometer readings equals 3 mm (in total); the maximal error for the measurement of the reference point is 1 mm, and the maximal total measurement error on the displacement therefore equals 4 mm.



The settlements were monitored using measuring bolts, which were placed on the edges of each of the surrounding buildings (for the larger buildings, additional measuring bolts are placed in between). The accuracy of these measuring bolts equals 1 mm. In addition to these measuring bolts, prisms (at least four) were placed on each building, and their displacements were measured by a total station (like the top displacement of the walls).

## MEASUREMENT RESULTS

### Straight Walls

The displacements measured near the center of the straight diaphragm walls are provided in Figure 10. The displacements before draining the pit are indicated by a dashed line, and the displacements after draining by a solid line.

The figure demonstrates that the results for both sides are similar to each other, which is to be expected due to the symmetry of the excavation. The effect of the draining is also clearly visible; because of this action, the maximal deflection of the wall increases from 6.3 mm to 9.3 mm.

An effect that is rather strange at first sight is the fact that the top of the diaphragm wall moves inward. This was not expected based on the different calculations that happened prior to the execution of the construction. Since the displacement of the top was measured by a total station with an accuracy of 1 mm, this displacement of about 4 mm cannot be attributed solely to an inaccuracy of the measuring equipment. The fact that the walls on both sides show this behavior (from independent measurements) seems to exclude the possibility that this was caused by a wrong measurement.

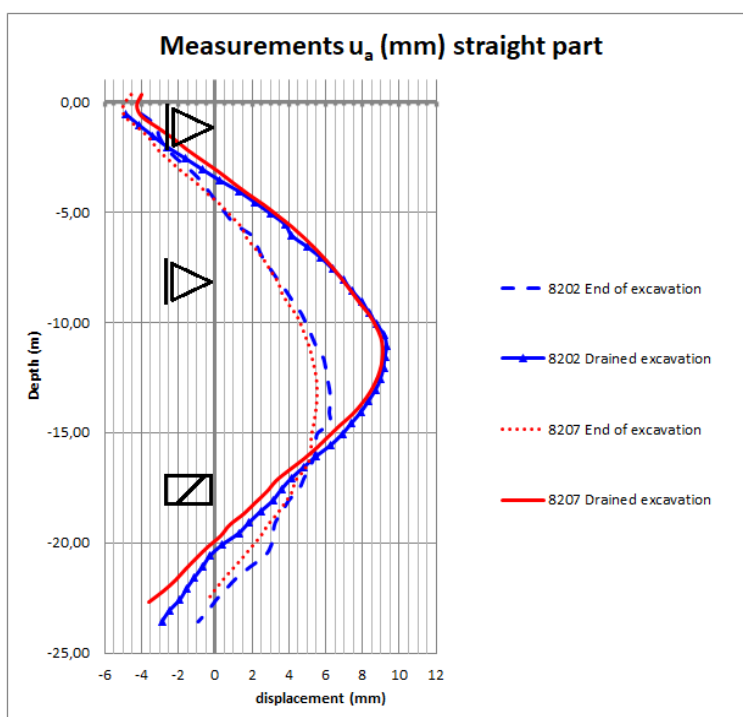


Figure 10. Displacements measured near the center of the straight diaphragm walls.

### Curved Walls

The displacements perpendicular to the wall are given in Figure 11. This figure shows both the results in the center of the curved part and those in the transition zone.

Initially, the results in the transition zone seem to be as expected and consistent with those in the straight part. However, the extra displacements—due to the draining of the pit—are clearly visible and the displacement of the top indicates a movement

into the soil instead of a displacement towards the pit. It is also remarkable that the displacement before draining is almost entirely negative.

The displacements in the center of the curved part seem to behave very strangely, and the highly irregular shape of the displacement line seems to indicate that something went wrong during the measurement. The trend-line of the measurements gives a much more likely displacement profile. Especially striking is the large relative displacement of the uppermost 2 m of the wall, which is highly unlikely. This also suggests that something might have gone wrong with the measurement. Taking the location of the measurement into account (it was right in front of the excavation of the entrance), it is presumable that the measuring equipment was damaged in some way. These measurements also show that the wall is moving even further into the ground after draining the pit, which is another peculiar observation. This could again be attributed to a faulty measurement of the top displacement, which served as a reference point for the entire displacement curve. As a result of all the aforementioned points, to draw conclusions for the rest of the excavation, the results in the center of the curved part should be used with precaution or perhaps not at all.

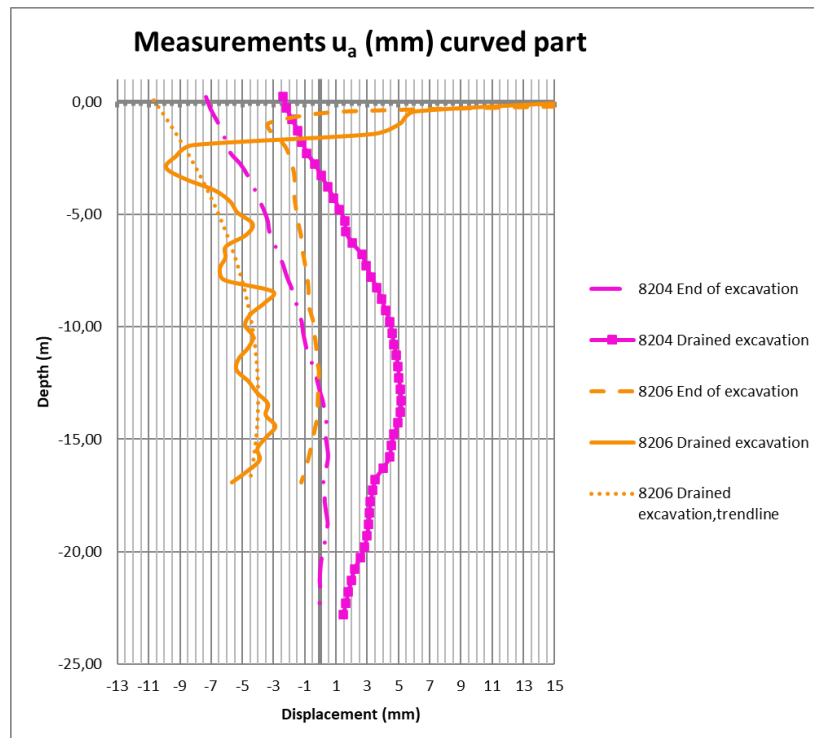


Figure 11. Displacement of the diaphragm walls in the curved section of the excavation.

## Settlements

The measured settlements after draining the pit are shown in Figure 8. This figure shows that the highest settlements are found at the synagogue and the building at the south-eastern edge of the Garenmarkt.

The settlements at the synagogue (maximal value of 18.3 mm) can be attributed for the most part to the excavation of the parking garage itself, due to its proximity to the straight walls. It is in the zone behind these walls that the highest calculated settlements were found. This effect can also be seen at the buildings further to the southwest. Here, the settlements also become higher for the buildings that are situated closer to the center of the straight part of the excavation. The settlements are of course a lot less pronounced for these buildings than for the synagogue, since they are further removed from the excavation.

The largest settlements (maximal value equal to 23.6 mm) can be found near the building at the intersection of the Garenmarkt and the Korevaarstraat (southeast on the figure). This can be attributed mainly to both the proximity to the excavation (although the building sits near the curved part with lesser expected settlements) and the excavation of the entrance. Due to



the large difference in settlements as compared to the buildings next to it (for which a similar effect due to the excavation itself is expected), the large value is presumably (for the most part) a result of the entrance, which is constructed on two sides of the building. This entrance is constructed with sheet piles which have a much smaller stiffness than the diaphragm walls.

For the other buildings around the Garenmarkt, the settlements are below 2 mm.

## COMPARISON OF MEASUREMENTS AND PRELIMINARY CALCULATIONS

### Straight Walls

Since the displacements on both sides of the straight part of the excavation are shown to be quite similar, the choice was made to compare the calculations with the measurement of only one location (to increase readability of the Figure 13). For simplicity, only the final results are considered.

For the straight-walled part of the excavation, the measured and calculated displacements are shown in Figure 12. In order not to overload the figure, only the best prediction (the PLAXIS 3D calculation) is shown. For comparison with other methods (which appear to be less accurate), the reader should check the section regarding the different calculations (Calculated Displacements in DESIGN CALCULATIONS).

From the aforementioned Figure 13, three main observations can be made:

1. While the calculations suggest that the top of the wall should move towards the excavated space, the measurements seem to indicate a movement of the top towards the soil-side;
2. The general shape of both calculations and measurements is rather similar; and
3. The maximal value obtained by the measurements (9.3 mm) is less than half of the value found in the most accurate calculation (23.3 mm).

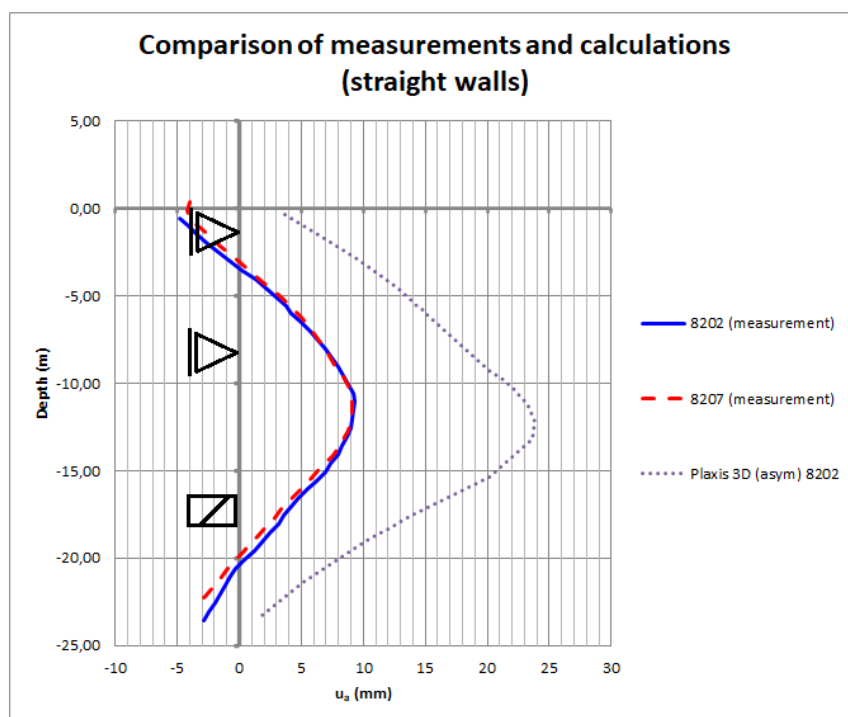


Figure 12. Comparison of the measured and calculated displacements near the center of the straight-walled part of the excavation.





## Curved Walls

Figure 13 shows both the measured and calculated displacements in the center of the part with curved walls. In the analysis of the measurements themselves, it became clear that the measurements were strange, if not altogether wrong. This was due to the large displacement of the top of the wall as compared to the rest of the wall as well as the very uneven form of the displacement curve.

When these strange measurements are compared closely to the calculations, it can be observed that:

1. While the uneven measured shape is unrealistic, the trend-line of the displacement appears similar to the calculations (both the three- and two-dimensional FE calculations), albeit only shape-wise;
2. The large relative movement of the top of the wall that was measured (and deemed rather unrealistic as well) is not visible in the preliminary calculations, although the asymmetrical PLAXIS 3D model does show a relative forward movement of the top of the wall (but a much smaller motion than the measurements show); and,
3. The entire wall would move inwards based on the measurements, yet the calculations predict a (small) outward movement.

Considering all the above, it is reasonable to think that the upper part of the measuring equipment was damaged during construction, resulting in the large top displacement (both absolute and relative to the other parts of the wall) and leading to a measurement that indicates that the wall moves into the soil. Omitting the top readings, and therefore also the fixed point of the curve, would allow us to shift the curve and gain an agreement between the measurements and calculations (or at least the trendline of the measurement).

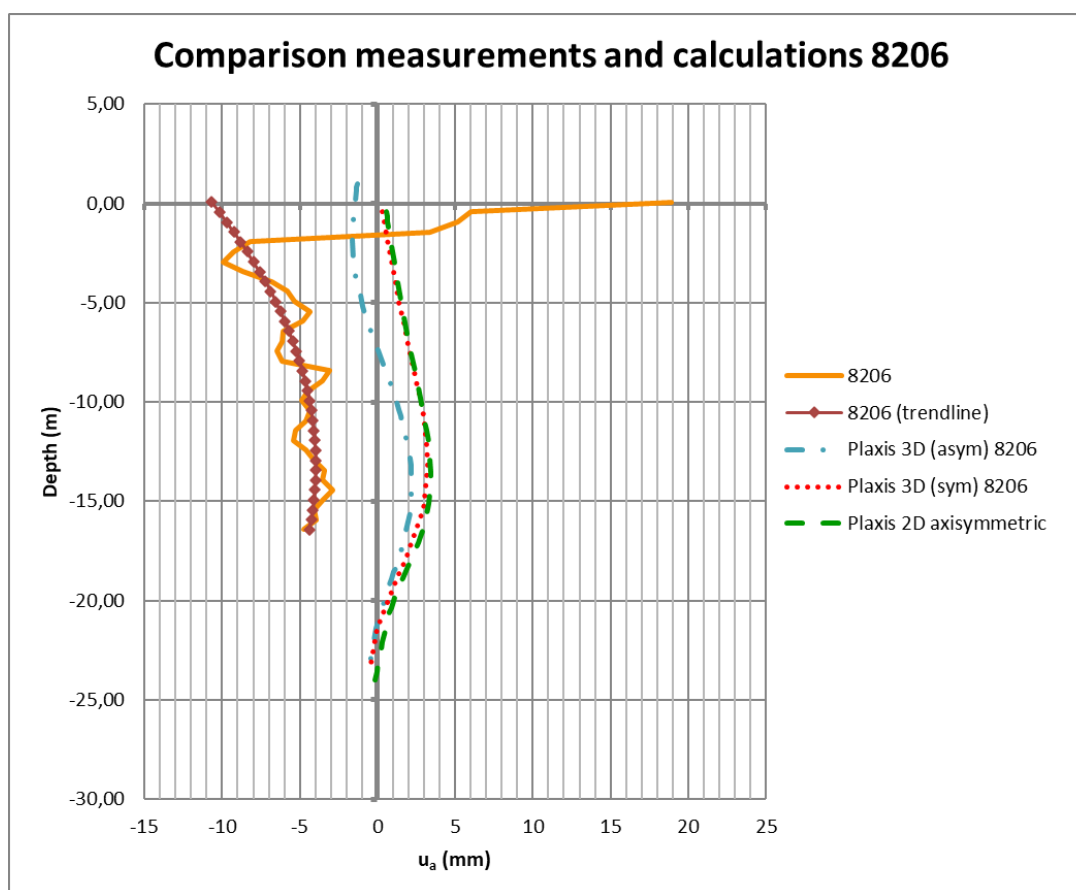


Figure 13. Comparison of the measured and calculated displacements near the center of the curved part of the excavation.



Now that the analysis is made for both the curved and straight walls, it is time to examine the transition zone. Both the measured and calculated displacements in the transition zone are provided in Figure 14.

Once again, the displacement of the top of the wall was towards the soil-side, while the calculations all indicated movements towards the excavated side. Compared to the calculations, the maximal measured displacement was larger than initially predicted. This difference is in the range of one to two millimeters, and therefore well within the accuracy range of the used measuring equipment. Since the maximal measurement error at the top is only 1 mm, measurement errors cannot be the only cause for the soil-faced movement of the top of the wall that was measured.

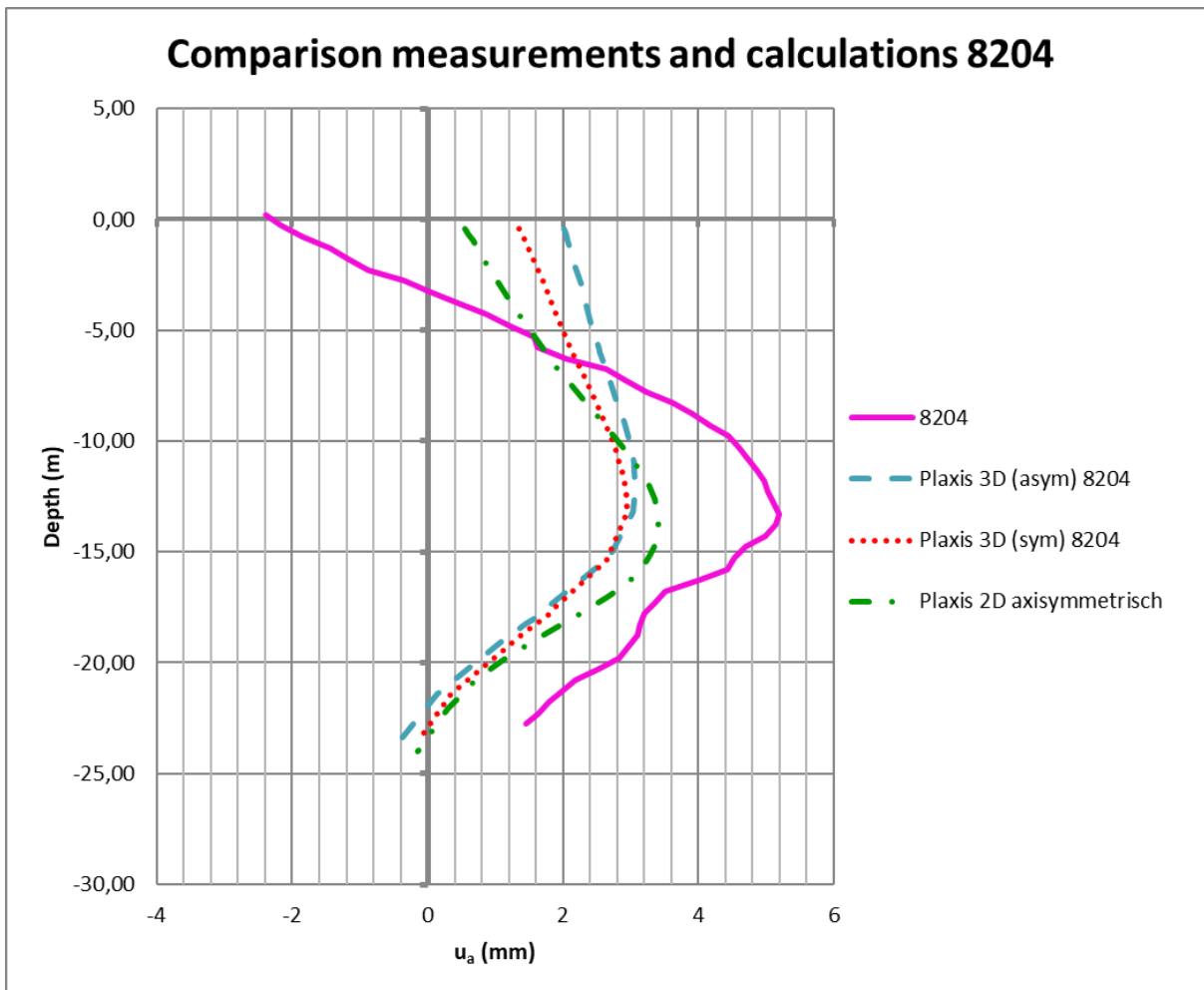


Figure 14. Comparison of the measured and calculated displacements in the transition zone in between the curved and straight parts of the excavation.

## Settlements

Figure 8 shows the calculated settlements (split into their three components) and the measured settlements measured on the front of the buildings around the Garenmarkt.

The largest values are found at the synagogue and the building located at the edge of the Garenmarkt and the Korevaarstraat. Near the synagogue, the predictions are rather accurate. All measured settlements are lower than the calculated ones (albeit barely in some places). This means that the calculations lead to a safe design.



The only place where the calculations underestimate the measurements is at the building in the lower right of the figure 9. This can most likely be attributed to the way the effect of the excavation of the entrance was calculated. This was done using a two-dimensional model, which was a correct approach for most buildings in the proximity of the Korevaarstraat road, since the excavation is situated only on the front side of the respective building. For this particular building, however, the excavation happened both in front of the building and along one of its sides, meaning a larger settlement can be expected.

The belief that the entrance is the reason for the larger settlements is strengthened by the fact that the two other types of settlements can't explain the difference. First, it cannot be explained by the excavation of the large building pit, since it is close to the curved part where small deformations were both calculated and measured. Secondly, it cannot be explained by the conservative estimate done by the contractor of the settlements caused by the sewage system works, since this estimate was indeed very conservative on all other places (e.g., on the right of figure 9 and on the buildings in the top left). Thirdly, the excavation of the entrance caused about 60 percent of the calculated settlement, and deviations of this calculation would have the largest impact.

Finally, we observe that the zones where the settlements caused by the large excavation are dominant (like at the lower left of the Figure 9), measured settlements are lower than the calculated ones. This is in line with the observation that the movement of the diaphragm wall that was measured was lower than the calculated value (especially for the straight walls).

### **Conclusions about the Comparison of Measurements and Calculations**

Regarding the horizontal displacements of the walls, the following conclusions can be formulated:

1. The measurements at the center of the curved part are most likely faulty, which can be deduced from the very uneven shape and strange behavior at the top, the general shape (visualized by using a trendline) seeming realistic but the absolute values being likely wrong. This is possibly caused by damage induced during construction of the entrance.
2. The reliable measurements seem to show that the top of the diaphragm wall is pressed into the soil instead of coming forward into the excavated space. This phenomenon appears for both measurements at the straight wall and also for the measurement in the transition zone (in the curved zone, the wall also moves backwards but, as already mentioned, the correctness of this measurement is doubtful). Although the calculation seemed to predict otherwise, this movement appears to have actually occurred.
3. In the transition zone, the difference between measurement and calculation is within the accuracy range of the measuring equipment, with the top displacement being an exception.
4. Although measurements and calculations for the straight walls are similar shape-wise, the absolute values differ. The measured values of the maximal displacements are about half (for the calculation method with the best similarity) to one third (for the least accurate calculations) of the calculated values.

Regarding the settlements, the following observations were made:

1. In zones where the settlements were mainly caused by the excavation of the parking garage itself, the measurements were lower than the calculations. This strengthens the hypothesis that the horizontal displacement of the diaphragm walls (especially in the straight parts of the walls) is smaller than initially calculated.
2. In nearly all locations, the calculated values are fairly similar to the measurements or result in a safe design.
3. The only zone where the settlements were not anticipated correctly (or at least a safe estimate was made) was the building on the edge of the Garenmarkt and the Korevaarstraat. This discrepancy can most likely be attributed to the model that was used to estimate the effect of the excavation of the entrance and not the model of the actual excavation of the parking garage.
4. Although the settlements give a general idea about the correctness of the models, they are less suited for a back-analysis than the horizontal displacements, since the result is also largely dependent on the execution of the works on the sewers, the entrance, and the precise state and type of the foundations of the nearby buildings.



---

## BACK-ANALYSIS OF THE MEASUREMENTS

### Goal and Method of the Back-Analysis

After the comparison of the measurements and the preliminary calculations, evidently there is a discrepancy between the values of the two. Therefore, an attempt was made to adapt the calculation model in such a way to ensure both the measurements and calculations are more closely aligned. The changes to the model were chosen in such a way that it should be possible to make these choices beforehand (meaning during the actual design of the construction) without being potentially unsafe. It was not the intention to improve agreement with changes that can only be known by hindsight.

To limit the collection of possible changes, a sensitivity analysis was done as a first step to rule out effects that do not have much of an influence. Even if the effect of a change is not significant, it is still relevant information since it means that, for the future design of similar constructions, these factors should not be considered in too much detail.

The back analysis is, for the sake of simplicity, focused on the straight walls, because (1) the measurements for the straight part are the most reliable, and (2) the displacements in the straight part are the largest, and therefore are normative for both the largest settlements (resulting from the actual excavation of the pit itself) and the deflection of the diaphragm walls.

For the analysis, a two-dimensional PLAXIS model was used (a three-dimensional model would make the analysis rather complex). The results of the measurements can't be used directly as the "goal" for the optimization process since the two-dimensional model did not take the edge effects (and so forth) into account; the measurements were therefore divided by the PSR of 0.875 (the ratio of the PLAXIS 3D results to the PLAXIS 2D results). These new values were smaller than the values that a "perfect" plane strain model would find. Possible inaccuracies in the measurements should also be considered (in this case, 4 mm divided by the PSR); consequently, the maximal displacement found by the improved model should be between 10.6 mm and 15.2 mm (10.6 mm would be the value with perfect measuring accuracy; lower predictions are unsafe and therefore undesirable).

### Sensitivity Analysis

The sensitivity analysis was carried out according to the aforementioned procedure. The following collection of influence factors (each accompanied by a short explanation) was considered for this analysis:

1. Modeling of the diaphragm wall: For the diaphragm wall, the most straightforward approach would have been to just make it a "line" in the 2D model with the unit mass of concrete. This is not entirely correct since PLAXIS superposes the plate on the soil, meaning that the weight of the plate for the software is actually the sum of its own and the soil, which is a common mistake according to Gouw (2014). To simplify, a value of 18 kN/m<sup>3</sup> is subtracted from the weight of the concrete. This is a safe simplification since it is less than the saturated weight of almost all soil layers. Also, the line shape is not entirely correct (although safe) since the end bearing of the plate is not accounted for (it can be taken into account by more recent PLAXIS versions, but not the one used for this analysis); a workaround for this is to model the plate with a "T" at its lower end, modeling the width of the wall to approximate the end bearing.
2. Young's modulus of the diaphragm wall: The simplest way to define the stiffness of the wall is to use a uniform value for Young's modulus  $E$ . For  $E$ , multiple choices are available. First of all, the uncracked value could be used (in this case, 25 GPa), but this would be too optimistic. Another option is to use a cracked  $E$  modulus (here, a value of 15 GPa is considered), yet this might be conservative. The best solution would be to make  $E$  a variable over the height of the wall depending on the local bending moment and the  $M$ - $\kappa$  curve of the wall. For the most modern PLAXIS version, this curve can be set as a material characteristic; for the used version, this is an iterative procedure carried out manually.
3. Stiffness of the soil: To quantify the effect of a general stiffening of the soil (for example, because a different method can be chosen to determine the parameters of the soil), the five parameters that determine the displacement in the HS Small model ( $E_{50}$ ,  $E_{ur}$ ,  $E_{oed}$ ,  $G_0$ , and  $\gamma_{0.7}$ ) were increased and decreased. The three  $E$ -moduli were all multiplied by the same factor (ranging from 0.5 to 2), while the new value for  $G_0$  was determined by the curve of Alpan (1970).  $\gamma_{0.7}$  was found by using the relation of Hardin and Drnevich (1972). These are the same methods as used in the original calculations.



4. Different soil profiles: For the design of the excavation, one single soil profile was used. Since this profile should result in a safe design, it is inherently a mixture of the worst soil characteristics that can be found in the vicinity of the excavation (to a reasonable degree, of course). To examine the influence of this decision, the calculations were redone using a cone penetration test (indicated as DKM3), which was performed very close to the location where the measurements for the straight wall were taken and was therefore more representative for the soil conditions than the general profile for the entire site. This should result in lower displacements since this test has less silty sand layers and more dense sand layers than the general design profile.
5. Surface loads: The highest surface load placed next to the excavation in the model equals 20 kPa, which is a safe assumption to cover the situation when large machinery is present next to the pit. The sensitivity of the result for removal of this load was checked.
6. Pile foundations of nearby houses: Some of the buildings around the square are placed on pile foundations, which can serve as some sort of soil nailing for the soil behind the wall if the piles are placed sufficiently close. A model was made that also took the house behind the wall and its pile foundation into consideration, and the piles were modeled according to CUR 228 (Beurze and Feddema 2010).
7. Connection between wall and struts: The most convenient way to model the struts was by using a linear spring. Inherent to these springs is the fact that they don't limit any rotation at their ends. For the temporary steel struts (in the middle), this way of modeling seemed sufficiently close to reality. However, for the top level this was not the case. As stated before, the upper struts were the concrete beams that would have to carry the roof and were cast in one piece with the top of the wall. Therefore, a clamped end of the strut appeared to be more reasonable here. This was achieved by modeling the beams as a plate with a clamped connection to the wall. The stiffness of this equivalent plate was that of one strut divided by the interdistance of the struts.

Table 3 gives an overview of the effects of the seven studied factors. The following effects are given:

- $u_{a,max}$ : The maximal horizontal displacement perpendicular to the wall.
- $N_{max}$ : The maximal normal force in the three struts (given per meter).
- $M_{max}$ : The maximal occurring bending moment in the diaphragm wall.

When factor 1 (modeling of the wall) is considered, the following abbreviations are used:

- $w$ : Calculated with the full weight of the wall (25 kN/m<sup>3</sup>).
- $w'$ : Calculated with the reduced weight of the wall (25 kN/m<sup>3</sup> -  $\gamma_{soil}$ ).
- $T$ : T-shaped bottom end to take into account the end bearing.

The following factors appear to have a major effect on the behavior of the walls:

- Not using a single value of EI for the diaphragm wall, but instead a value that varies depending on the bending moment in the wall (based on the wall's M- $\kappa$  curve).
- Using the specific soil layers at the studied location instead of a general profile for the entire excavation. Although this approach is convenient for this study since only one location was considered, it becomes rather cumbersome for the actual design of an excavation and some sort of generalization will always have to be made regarding the soil profile to keep the amount of work reasonable. However, this result does show that in a search for optimization, a more precise discretization of the soil layers could be useful.
- Modeling the roof-beams with a clamped connection to the wall (instead of a simple spring with a hinge at its end).



- Modeling the wall with its reduced self-weight and a “T” at the bottom. In this case, the effect of this change is lesser than the three factors mentioned above, yet the reasoning behind this change is sound and it could result in a more economical design.

The following factors appear to have only a limited effect (or are at least not considered for the back-calculation):

- Increasing the stiffness of the soil. The soil has to become stiffer, and much so, before a significant effect is observed.
- Modeling the pile foundations of nearby houses. Although it might have an effect in some cases, it did not have much effect for the Garenmarkt. The reason is that the piles were not located in the influence zone (deformed soil mass) of the excavation. Hence, the movement of the soil was not obstructed by the piles.
- Removing the surface load. It makes sense that the effect of a load of 20 kPa is not that large for an excavation of about 20 m deep. The design is not very sensitive for this load.

*Table 3. Overview of the results of the sensitivity analysis.*

Factor $n^{\circ}$	Details of Change	Value			Relative difference with original [%]		
		$u_{a,max}$ [mm]	$N_{max}$ [kN/m]	$M_{max}$ [kNm/m]	$u_{a,max}$	$N_{max}$	$M_{max}$
-	Original model	24.11	1120	1224	-	-	-
1	w'+T	22.95	1093	1202	-4.8	-2.4	-1.8
1	w+T	25.71	1139	1234	+6.6	+1.7	+0.8
1	w	31.13	1263	1452	+29.1	+12.8	+18.6
2	$EI_{wall}$ function of M	22.42	1111	1222	-7.0	-0.8	-0.2
3	$E_{soil} \times 0.75$	25.23	1134	1247	+4.6	+1.2	+1.9
3	$E_{soil} \times 1.25$	22.90	1106	1187	-5.0	-1.2	-3.0
4	profile DKM3	20.50	1056	1119	-15.0	-5.7	-8.6
5	no surface load	24.09	1120	1220	-0.1	0.0	-0.3
6	piles of nearby building modeled	23.99	1109	1228	0.5	-1.0	+0.3
7	upper struts clamped	21.59	1063	1221	-10.5	-5.1	-0.2

### Optimization of the Model

The four changes mentioned in the conclusion of the sensitivity analysis have been applied to the two-dimensional calculation model. The displacements and bending moments of the diaphragm wall are given in Figure 15 and Figure 17.

As expected, the deformations become smaller when applying these changes, although they are still larger than the measurements (including the range of measuring inaccuracies) when the clamped connection at the top is not considered. When this connection is considered, the maximal displacement is 11.92 mm, which is within the desired range. The problem with this adaption is the shape of the displacement curve at the top; the clamped connection induces an extra bend in the wall which is not found in any of the measurements.

A possible way to “remove” this problem is by introducing a temperature change in the upper struts (Figure 16), which is done both for the case of a clamped connection and the original connection modeled by a spring. This does indeed solve the problem of the shape but, in order to do so, a temperature change of about 30 °C is needed, which is pretty unlikely to have occurred since our measurements were done in December (when the daily temperature average was 6.1 °C). Although a temperature change does not solve the discrepancy entirely, it may be accountable for some part of it.

Finally, the bending moments in the wall are analyzed. For most changes to the model, the difference was not that big although the calculated bending moments become slightly smaller in the optimized models. This was to be expected since the varying value of EI based on M makes the bending moment “spread out” more over the height of the wall. In Figure 18, a dashed line



is added which provides the value of  $M$  when the first cracks start to appear. This value is rarely exceeded, meaning that using the value of 15 GPa for Young's modulus is really too conservative.

Modeling the connection with the upper struts as a clamped connection is impactful since it significantly changes the bending moments in the upper part of the wall (the bending in the upper part of the wall does not have to be zero anymore) and lowers (although less significantly) the value in the central part.

This makes it rather difficult to assess if the clamped connection is necessary in the back-calculation. It could be conservatively omitted when only displacements are the desired output of the calculation. On the other hand, it could result in underestimating the forces in the wall. A torsional spring would be most appropriate to model the connection. This has not been considered in this paper, but it is clear that the modeling of the connection plays an important role in the obtained results.

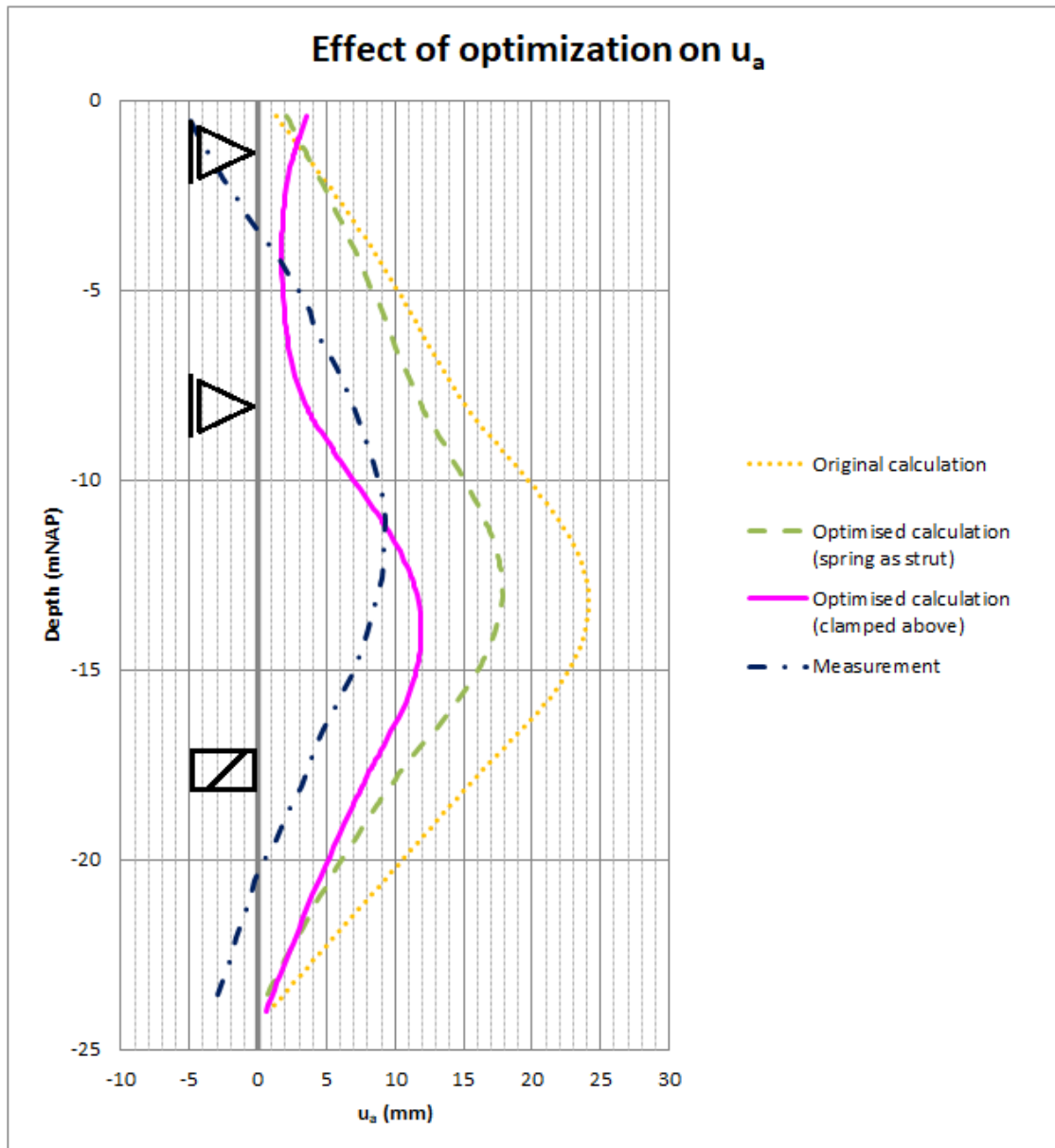


Figure 15. Horizontal displacements perpendicular to the wall after applying the proposed changes to the model.

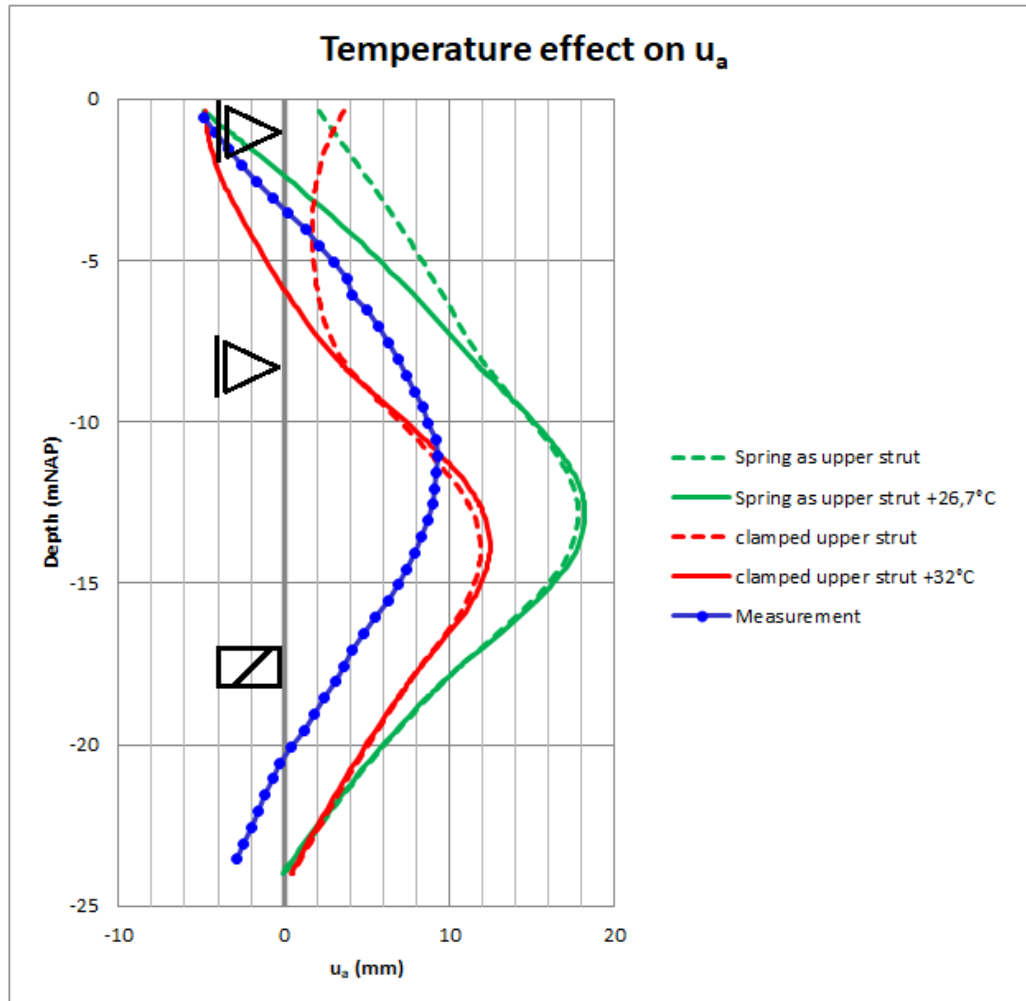


Figure 16. Displacements after applying a temperature raise on the upper struts.

## CONCLUSION

In this paper, the measurements of the diaphragm wall displacements for a deep excavation were studied. The comparison of the design calculations and measurements show that the latter are more conservative. Subsequently, an attempt was made to improve the correctness of the predictions by means of a back-calculation.

As a first step of this improvement, a sensitivity analysis was carried out to check which effects had a major impact on the calculated results. Secondly, the most important changes from the sensitivity analysis were applied to find a model that better agreed with the measurements. For future designs of similar, deep excavations, it is advisable to take the following suggestions into account:

1. Choose an appropriate way to model the soil (HS Small should generally give the best prediction). Identify for the chosen model which constitutive parameters have the most influence on the results and pay special attention to those.
2. Adapt the bending stiffness of the diaphragm wall to the bending moment at that location of the wall (instead of using a uniform, safe value for the entire wall).
3. Use the specific soil profile at the location instead of a general profile for the entire excavation; this is of course not always practicable, so this advice should be read as “discretize as much as possible.”



4. Subtract the weight of the soil from the unit weight of the wall, otherwise it will be counted twice. Also, the end bearing should be considered (this can be done with either a “T” shaped foot or the specific end bearing value, depending on the calculation software used).
5. Give special attention to the connection between a clamped strut and the wall; using a spring might be conservative from the point of view of the displacements but can underestimate the bending moments in the wall (a torsional spring could be the answer but is not considered in this paper).

Applying these five changes did show a greater alignment between measurement and calculation results for this particular case, although it is still not perfect (especially the movement of the top of the wall). A part of the discrepancy could be explained by temperature effects, but they certainly don't explain it entirely.

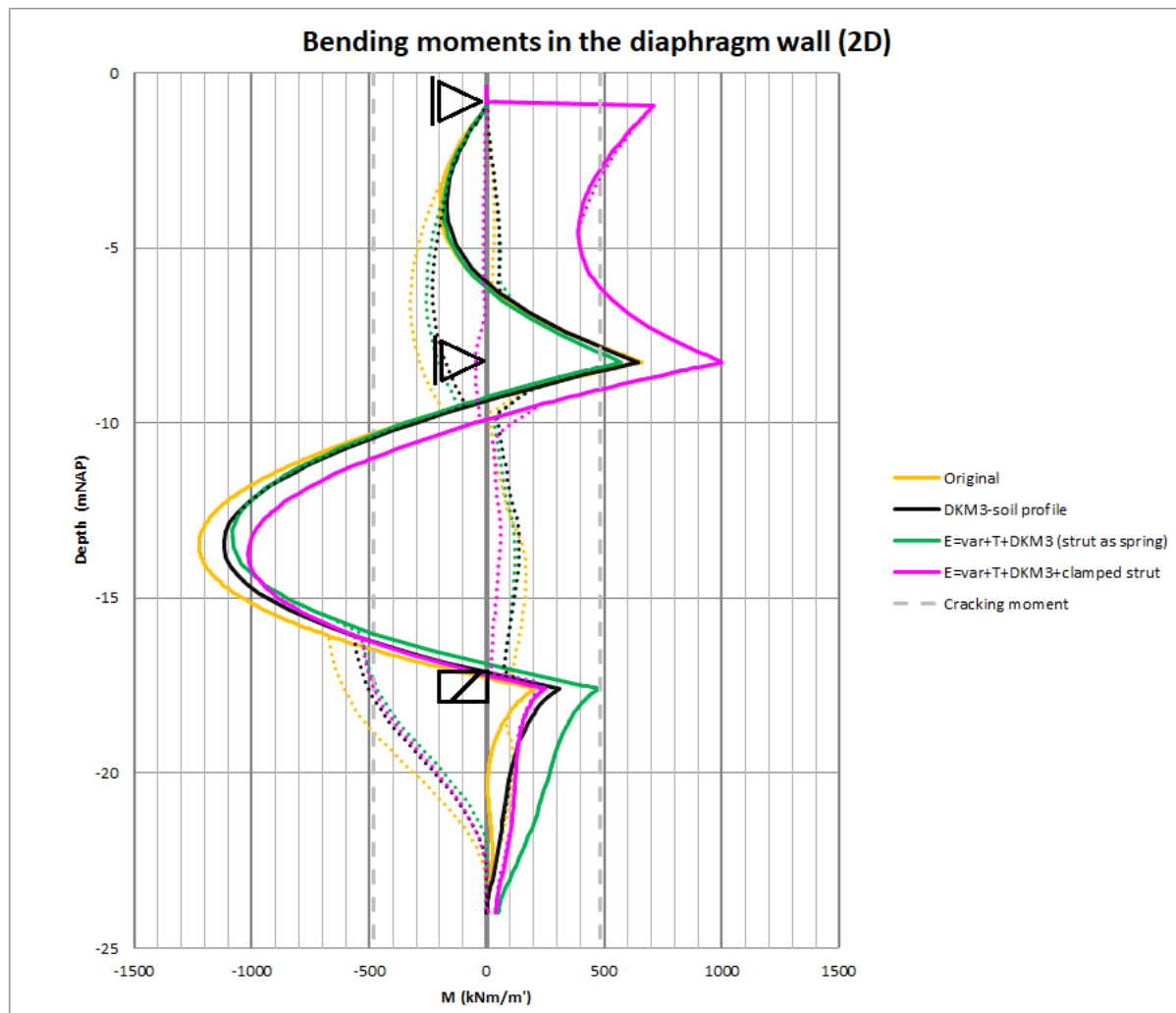


Figure 17. Bending moments in the diaphragm wall for the different changes; the dotted lines indicate the moment envelope.

## ACKNOWLEDGMENTS

The authors gratefully acknowledge the joint venture “Combinatie Parkeergarages Leiden Dura Vermeer – BESIX” for the use of the data presented in this study.



---

## REFERENCES

- Alpan, I. (1970). "The geotechnical properties of soils." *Earth Science Reviews*, 6(1), 5-49.
- Beurze, R. S., and Feddema, A. (2010). "CUR 228, ontwerprichtlijnen 'Door grond horizontaal belaste palen'." *Geotechniek* (Funderingsdag special), 10-14.
- Burland, J. B., and Wroth, C. P. (1974). "Settlement of buildings and associated damage." *Proc. of the British Geotechnical Society's Conference on the Settlement of Structures, Cambridge, Session 5: Allowable and differential settlement of structures, including damage and soil-structure interaction*, 611-654.
- Clough, W. G., and O'Rourke, T. D. (1990). "Construction induced movements of in situ walls." *Geotechnical Special Publication*, 439-470.
- Creten, S. (2020). "Analyse van de metingen en terugkoppeling aan de berekeningen voor een diepe, ondergrondse parkeergarage" [Master's thesis, KU Leuven].
- Gouw, T. L. (2014). "Common mistakes on the application of PLAXIS 2D in analyzing excavation problems." *International Journal of Applied Engineering Research*, 9(21), 8291-8311.
- Hardin, B. O. and Drnevich, V. P. (1972). "Shear modulus and damping of soils: design equations and curves." *Journal of Soil Mechanics and Foundations Division*, 98(SM7), 667-692.
- Hsiung, B. B. and Dao, S. (2014). "Evaluation of Constitutive Soil Models for Predicting Movements Caused by a Deep Excavation in Sands." *Electronic Journal of Geotechnical Engineering*, 19, 17325-17344.
- Korf, M., Roggeveld, M. P. et al. (2012). "F530: Aanbevelingen voor het ontwerp van bouwkuipen in stedelijke omgeving." *Technical report*, COB, 582 2600AN Delft, the Netherlands.
- Long, M. (2001). "Database for retaining wall and ground movements due to deep excavations." *Journal of Geotechnical and Geoenvironmental Engineering*, 127(3), 203-224.
- Moorman, C. (2004). "Analysis of wall and ground movements due to deep excavations in soft soil based on a new worldwide database." *Soils and Foundations (Japanese Geotechnical Society)*, 44(1), 87-98.
- op de Kelder, M. A. (2015). "2D FEM analysis compared with the in-situ deformation measurements: A small study on the performance of the HS and HSsmall model in a design." *Plaxis Bulletin*, 2015 (autumn), 10-17.
- Ou, C. Y., Chiou, D. C., and Wu, T. S. (1996). "Three-dimensional finite element analysis of deep excavations." *Journal of Geotechnical and Geoenvironmental Engineering*, 122(5), 337-345.
- Rooduijn, M. P. (2010). "Bouwkuip van project Le Carrefour te Leiden (deel 1)." *Geotechniek*, 13(4), 48-51.
- Rooduijn, M. P. (2010). "Bouwkuip van project Le Carrefour te Leiden. Evaluatie van metingen en analyses (deel 2)." *Geotechniek*, 14(1), 34-37.
- Skempton, A. W., and MacDonald, D. H. (1956). "The allowable settlements of Buildings." *Structural Paper*, (50), 727-761.

The open access Mission of the International Journal of Geoengineering Case Histories is made possible by the support of the following organizations:



Access the content of the ISSMGE International Journal of Geoengineering Case Histories at:  
<https://www.geocasehistoriesjournal.org>